2005

Influence of Isentropic Mixing on Seasonal Ozone Variations in the Lower Stratosphere and Upper Troposphere

Ping Jing
Loyola University Chicago, pjing@luc.edu

Derek M. Cunnold

ES Yang

HJ Wang

Recommended Citation

Jing, P., D. M. Cunnold, E.-S. Yang, and H.-J. Wang (2005), Influence of isentropic transport on seasonal ozone variations in the lower stratosphere and subtropical upper troposphere, J. Geophys. Res., 110, D10110, doi:10.1029/2004JD005416

Influence of isentropic transport on seasonal ozone variations in the lower stratosphere and subtropical upper troposphere

P. Jing, D. M. Cunnold, E.-S. Yang, and H.-J. Wang

School of Earth and Atmosphere Sciences, Georgia Institute of Technology, Atlanta, Georgia, USA

Received 2 September 2004; revised 24 January 2005; accepted 3 February 2005; published 26 May 2005.

[1] The isentropic cross-tropopause ozone transport has been estimated in both hemispheres in 1999 based on the potential vorticity mapping of Stratospheric Aerosol and Gas Experiment II ozone measurements and contour advection calculations using the NASA Goddard Space Flight Center Global and Modeling Assimilation Office analysis. The estimated net isentropic stratosphere-to-troposphere ozone flux is $\sim 118 \pm 61 \times 10^9$ kg yr^{-1} globally within the layer between 330 and 370 K in 1999; 60% of it is found in the Northern Hemisphere, and 40% is found in the Southern Hemisphere. The monthly average ozone fluxes are strongest in summer and weakest in winter in both hemispheres. The seasonal variations of ozone in the lower stratosphere (LS) and upper troposphere (UT) have been analyzed using ozonesonde observations from ozonesonde stations in the extratropics and subtropics, respectively. It is shown that observed ozone levels increase in the UT over subtropical ozonesonde stations and decrease in the LS over extratropical stations in late spring/early summer and that the ozone increases in the summertime subtropical UT are unlikely to be explained by photochemical ozone production and diabatic transport alone. We conclude that isentropic transport is a significant contributor to ozone levels in the subtropical upper troposphere, especially in summer.

Citation: Jing, P., D. M. Cunnold, E.-S. Yang, and H.-J. Wang (2005), Influence of isentropic transport on seasonal ozone variations in the lower stratosphere and subtropical upper troposphere, *J. Geophys. Res.*, *110*, D10110, doi:10.1029/2004JD005416.

1. Introduction

[2] Isentropic transport has been recognized as an important pathway for stratosphere-troposphere exchange (STE) [*Holton et al.*, 1995; *Dethof et al.*, 2000a, 2000b]. As opposed to the diabatic STE, in which air mainly moves upward at the equator and sinks in the extratropics, the isentropic STE moves quasi-horizontally along isentropic surfaces and crosses the extratropical tropopause in the "middleworld" [*Hoskins*, 1991]. This quasi-horizontal isentropic exchange occurs on a shorter timescale (days to weeks) than the diabatic STE (months to a year) [*Chen*, 1995], and the spatial scales of the isentropic STE vary widely from small scale (<200 km) to large scale (2000 $\sim$ 3000 km) [*Appenzeller et al.*, 1996]. The potential vorticities (PV) usually have strong latitudinal gradients on the isentropic surfaces which intersect the tropopause in the "middleworld," indicating that the isentropic transport is hindered around the tropopause because otherwise the strong PV gradients would be destroyed by vigorous mixing of stratospheric and tropospheric air [*Holton et al.*, 1995]. The PV gradients along the isentropes which cross the tropopause are weaker in summer than in winter in part because of the influence of summertime monsoon circulations and cutoff cyclones [*Price and Vaughan*, 1993; *Chen*, 1995; *Haynes and Shuckburgh*, 2000]. Consequently, the isentropic STE has been shown to be strongest in summer and weakest in winter [*Chen*, 1995; *Dethof et al.*, 2000a, 2000b]. Studies based on aircraft measurements [*Dessler et al.*, 1995; *Tuck et al.*, 1997, 2003] and a model study based on contour advection [*Dethof et al.*, 2000b] have suggested that the summertime increase of water vapor in the northern midlatitude lower stratosphere (LS) is associated with isentropic advection from the subtropical upper troposphere (UT) in the Northern Hemisphere (NH).

[3] While diabatic transport tends to sharpen the latitudinal ozone gradients at midlatitudes by dumping ozone-rich air at high latitudes and transferring ozone-poor air upward at the equator, the effect of isentropic transport is to reduce this latitudinal ozone gradient by exchanging ozone quasi-horizontally between the subtropics and the extratropics. Measurements taken by the Stratospheric Aerosol and Gas Experiments (SAGE) II, for example, have shown a decrease of ozone in the extratropical LS accompanied by ozone increase in the subtropical UT in late spring/summer [*P. H. Wang et al.*, 1998]. This suggests the possibility that isentropic transport could be a significant contributor to the ozone budget in the subtropical UT by spreading the stored ozone-rich air from the extratropical LS.

[4] Regarding the quantification of ozone STE, the diabatic ozone STE has been estimated since the 1960s [e.g., *Junge*, 1962; *Danielson*, 1968; *Gidel and Shapiro*, 1980; *Murphy and Fahey*, 1994; *Müller and Brasseur*, 1995; *Gettelman et al.*, 1997; *Olsen et al.*, 2002, 2003]. Estimates of the global net diabatic cross-tropopause ozone flux are

0148-0227/05/2004JD005416

Table 1. Sonde Data Used in the Analysis

Identification	Station	Latitude	Longitude	Period	Profiles
99	Hohenpeissenberg	47.8	11.0	1979–2001	2806
67	Boulder	40.0	−105.3	1979–2000	811
7	Kagoshima	31.6	130.6	1991–2001	401
190	Naha	26.2	127.7	1991–2000	408
256	Lauder	−45.0	169.7	1986–2000	974

between $400 \sim 500 \times 10^9$ kg yr^{-1}. On the other hand, the isentropic ozone STE has not been well quantified until a recent study by *Jing et al.* [2004]. On the basis of contour advection and the correlation between ozone mixing ratio and potential vorticity, *Jing et al.* [2004] estimated the isentropic cross-tropopause ozone fluxes between 330 and 370 K in the NH. Their net stratosphere-to-troposphere ozone flux is estimated to be approximately 50×10^9 kg yr^{-1}. This indicates that from a global viewpoint, the isentropic ozone STE seems to be a smaller contributor to the total ozone budget in the troposphere than the diabatic exchange. However, the isentropic ozone transport from stratosphere to troposphere (S→T) in the NH mostly occurs around 30°–40°N latitude [*Jing et al.*, 2004] and the maximum diabatic S→T mass transport in the NH is located around 60°N latitude [*Schoeberl*, 2004]. Therefore the isentropic STE could be significant in controlling regional ozone levels in the subtropical UT. For example, ozone-rich laminae observed in the UT over the tropical Indian Ocean have been shown to be transported quasi-horizontally from the stratosphere near the subtropical jet stream [*Zachariasse et al.*, 2000]. High ozone anomalies derived from the Measurement of Ozone and Water Vapor by Airbus In-Service Aircraft (MOZAIC) observations occurred mostly in the subtropical North Atlantic and the Mediterranean, and they were shown to be coincident with filaments of isentropic transport from the stratosphere [*Morgenstern and Carver*, 2001]. It has been acknowledged that it takes ozone to produce ozone [*Davis et al.*, 2003] and thus the influence of this stratospheric source on the tropospheric ozone production could be amplified.

[5] *Jing et al.* [2004] have examined the magnitude and geographical distributions of the NH isentropic ozone flux across the tropopause. The purpose of the present study is to provide a global estimate of the isentropic ozone STE and to investigate its association with the seasonal ozone variations derived from ozonesonde observations in the LS/UT. As described by *Jing et al.* [2004], PV is used to define the tropopause and to distinguish between stratospheric ozone and tropospheric ozone, because PV is conserved in isentropic transport and has larger absolute values in the stratosphere than in the troposphere. By applying contour advection, the development of filaments on PV contours during the isentropic transport is well depicted, and the cross-tropopause transport ozone fluxes from troposphere to stratosphere (T→S) and from S→T are determined by calculating the amount of ozone within the filaments poleward and equatorward of the tropopause, respectively.

[6] Our quantification method follows the contour advection technique to estimate isentropic mass fluxes as given by *Dethof et al.* [2000a]. A recent study by *Schoeberl* [2004] used a different approach to estimate the isentropic mass flux by calculating the difference between the net cross-tropopause mass flux and the net diabatic cross-tropopause mass flux. His estimated adiabatic mass flux is always directed from T→S, which is in the direction opposite to that of the mass fluxes of *Dethof et al.* [2000a] based on contour advection. However, this does not necessarily mean that the two methods are in conflict.

[7] The isentropic mass flux given by *Schoeberl* [2004] is the bulk isentropic mass flux, which indicates mass fluxes along all the isentropic levels that cross the tropopause. The isentropic mass flux given by *Dethof et al.* [2000a] and the isentropic ozone flux given by *Jing et al.* [2004], on the other hand, are estimated only on isentropic surfaces between 330 and 370 K. According to *Seo and Bowman* [2001], using a Lagrangian method, their estimated net isentropic mass fluxes on 330 and 350 K are both from S→T except in late fall in the NH, and this is not inconsistent with the results of *Dethof et al.* [2000a]. In addition, the geographical distributions of the isentropic mass flux on 330 and 350 K given by *Seo and Bowman* [2001] are consistent with those of the isentropic ozone fluxes by contour advection [*Jing et al.*, 2004]; both the isentropic mass flux and the isentropic ozone flux preferentially occur over the Pacific and the western Atlantic Oceans and over northwest Africa. It is possible that the net mass isentropic flux below 330 K is directed from T→S. The isentropic surfaces below 330 K intersect the tropopause at higher latitudes, and air could be substantially transported from T→S along isentropic surfaces in subpolar regions via stationary waves in wintertime [*Hoerling et al.*, 1993].

[8] We think that the contour advection method should capture most of the isentropic exchange around the subtropical tropopause and it is reliable for studying isentropic transport along isentropic surfaces above 330 K. Isentropic

Table 2. Correlation Coefficients (R) Between PV and ln(O_3) in 1999[a]

	335 K		345 K		355 K		365 K	
Month	NH	SH	NH	SH	NH	SH	NH	SH
1	0.83	0.88	0.88	0.91	0.89	0.92	0.89	0.93
2	0.83	0.88	0.89	0.91	0.91	0.92	0.90	0.93
3	0.87	0.87	0.91	0.91	0.91	0.91	0.89	0.91
4	0.86	0.74	0.91	0.79	0.93	0.81	0.92	0.81
5	0.78	0.73	0.81	0.79	0.81	0.81	0.71	0.79
6	0.85	0.85	0.92	0.91	0.94	0.92	0.94	0.93
7	0.47[b]	0.89	0.55[b]	0.92	0.55[b]	0.91	0.47[b]	0.89
8	0.88	0.84	0.94	0.86	0.94	0.85	0.94	0.84
9	0.76	0.85	0.84	0.86	0.88	0.84	0.89	0.82
10	0.90	0.79	0.93	0.88	0.94	0.87	0.94	0.84
11	0.71	0.81	0.78	0.81	0.80	0.73	0.80	0.87
12	0.88	0.85	0.90	0.86	0.89	0.79	0.86	0.68

[a]NH is Northern Hemisphere; SH is Southern Hemisphere.
[b]Because of these small values of the correlation coefficients the PV and ozone relationships in the NH for June are used instead (see section 2.2).

Table 3. Differences Between PV-Mapped Ozone and Ozonesonde Data in 1999[a]

	Hohenpeissenberg N = 105			Boulder N = 40			Kagoshima N = 45			Lauder N = 52		
θ, K	μ, %	σ, %	R	μ, %	σ, %	R	μ, %	σ, %	R	μ, %	σ, %	R
365	6.9	29.4	0.85	3.9	39.5	0.89	13.1	25.0	0.91	1.8	21.1	0.91
355	5.2	32.5	0.86	1.3	36.6	0.92	13.7	25.4	0.91	2.3	22.4	0.88
345	−1.8	23.7	0.90	1.9	32.8	0.90	9.5	24.2	0.90	1.6	25.3	0.91
335	−10.3	27.7	0.87	−8.1	38.2	0.80	−0.5	24.9	0.87	−3.9	20.9	0.95

[a]N is the number of collected ozonesonde profiles; μ and σ are the median and standard deviation of their differences ((PV-mapped − sonde)/sonde), respectively; R is the correlation coefficient of the time series of PV-mapped ozone and ozonesonde data.

surfaces below 330 K do not always intersect the tropopause and the tropopause contour would thus not always appear on these surfaces. We therefore do not include the isentropic surfaces below 330 K in this paper.

[9] Section 2 describes the data and method used to diagnose isentropic ozone STE and assesses the accuracy of the PV/O_3 mapping. The principal results are presented in section 3, in which the isentropic ozone fluxes and its seasonality and interhemispheric differences are revealed. Section 4 reveals the seasonal variations of ozone from ozonesonde observations. A discussion and concluding remarks are provided in section 5.

2. Data and Method

2.1. Meteorological and Ozone Data

[10] This study employs Goddard Earth Observing System Version 3 (GEOS-3) assimilated products for 1999 from the Global Modeling and Assimilation Office (GMAO) at NASA's Goddard Space Flight Center, whereas our previ-

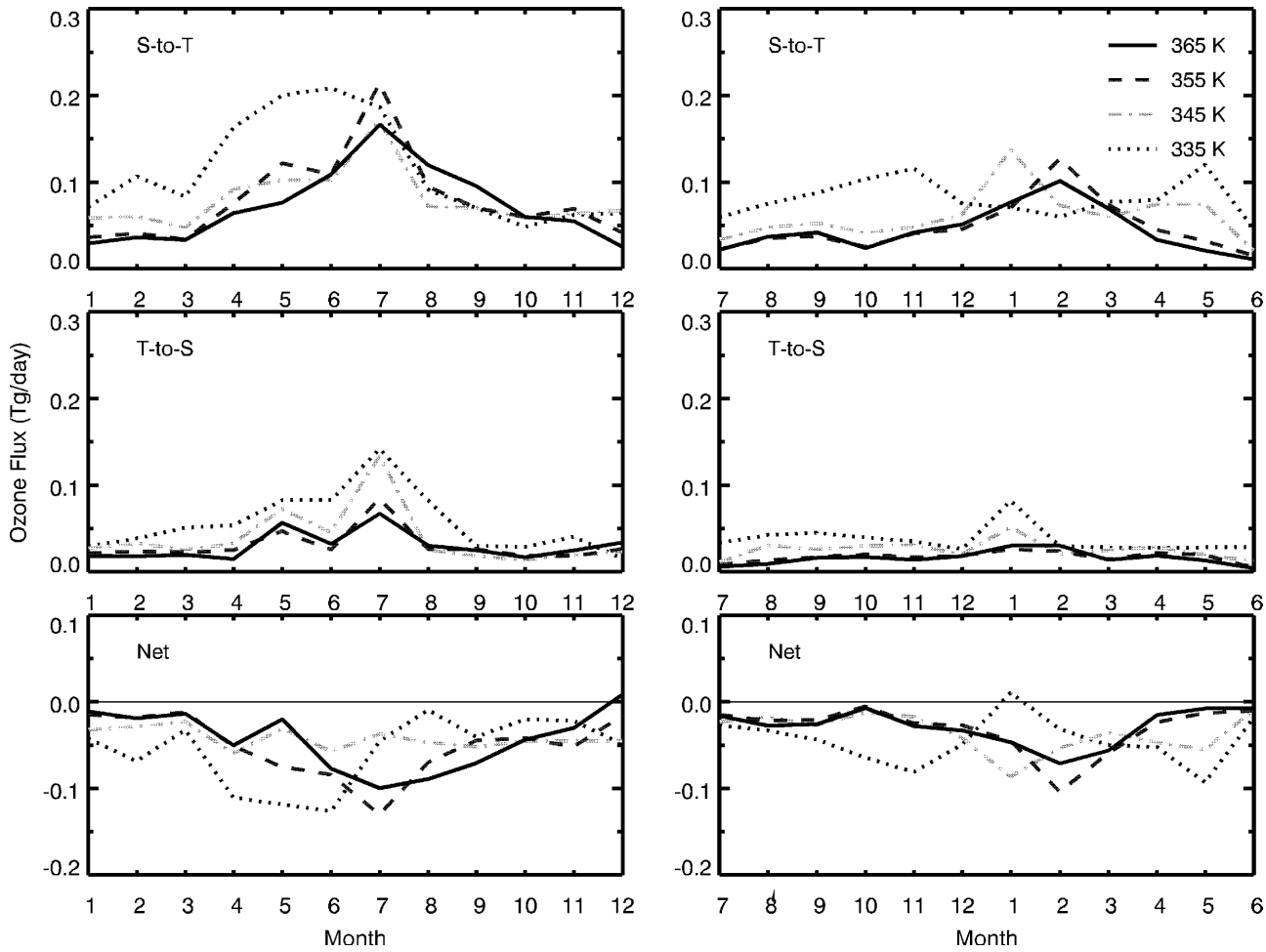

Figure 1. Estimated monthly average isentropic ozone fluxes (in Tg d^{-1}) (1Tg = 10^9 kg) across the tropopause in the Northern Hemisphere (NH) (left column) and Southern Hemisphere (SH) (right column) in 1999. Negative (positive) net fluxes indicate S→T (T→S) net ozone transport. Note that the *x* axis is shifted by six months in the SH.

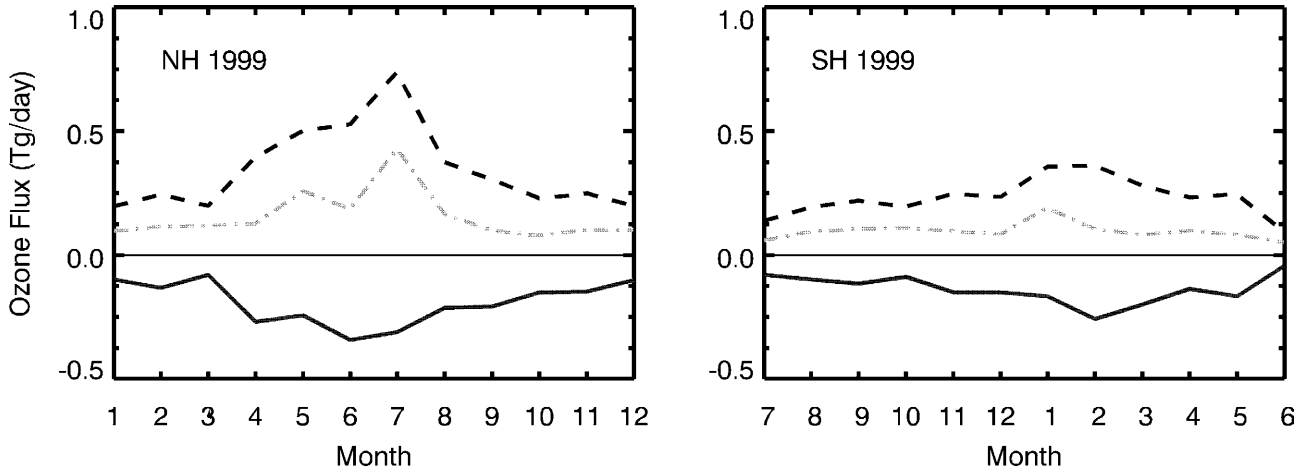

Figure 2. Estimated monthly average ozone fluxes after combining those fluxes on the four isentropic surfaces in Figure 1. Dashed lines represent S→T fluxes, dash-dotted lines represent T→S fluxes, and solid lines represent net ozone fluxes.

ous study [*Jing et al.*, 2004] used GEOS-1 products for 1990. The assimilated data fields are available every 6 hours with a horizontal resolution of 2.5° longitude by 2.0° latitude on 36 isobaric surfaces [*Data Assimilation Office*, 1997]. They were vertically interpolated onto nine isentropic surfaces from 330 to 370 K at 5 K resolution using the interpolation method of *Edouard et al.* [1997].

[11] The ozone data are from SAGE II measurements and ozonesonde observations. SAGE II has been continuously measuring ozone profiles since October 1984. Version 6.1 ozone retrievals have been used in this study even though they have large error bars at low altitudes; for example, a significant number of the profiles have reported retrieval errors of 300% below 13 km altitude. However, *Wang et al.* [2002] have shown that the set of measurements with less than 300% error bars have a mean bias of less than 10% down to the tropopause. Moreover, at 11 km altitude this set of measurements exhibits a distribution of variability similar to that from ozonesonde measurements at the same location [*Wang et al.*, 2002]. This suggests that the error bars are being overestimated. Figure 5a from *Wang et al.* [2002] clearly demonstrates that filtering the measurements using a more restrictive percentage error (e.g., 50%) will preferentially eliminate the smaller concentrations (which have less measured variance than larger concentrations) thus producing an undesirable upward bias in the means. Ozonesonde data were obtained from the World Ozone and Ultraviolet Radiation Data Center (WOUDC) for five stations: Hohenpeissenberg in Germany; Kagoshima and Naha in Japan; Boulder in the United States; and Lauder in New Zealand (Table 1).

2.2. Derivation of Daily Ozone Distributions From Monthly PV/O_3 Relationships

[12] The correlation between PV and ozone fields has been used to diagnose diabatic ozone STE for decades [*Danielson*, 1968; *Gidel and Shapiro*, 1980; *Danielson et al.*, 1987; *Morgenstern and Marenco*, 2000; *Olsen et al.*, 2002, 2003]. *Jing et al.* [2004] took advantage of the relationship between the two variables to derive daily ozone maps on isentropic surfaces for 1990. They had previously noted that PV was better correlated with $\ln(O_3)$ than with O_3 on isentropic surfaces and they assumed a linear relationship between PV and $\ln(O_3)$: $\ln(O_3) = \beta_0 + \beta_1 \cdot PV$. This is consistent with the fact that the linear fit between PV and ozone is different for different latitude bands as illustrated by *Waugh et al.* [1997], because the edge of the polar vortex and the tropopause would hinder the air from being well mixed between high and middle latitudes and between middle and low latitudes. Because the isentropic transport between these regions is rather random and sporadic, it is more consistent for us to use the PV/$\ln(O_3)$ fit than to try to develop PV/O_3 fits for different latitude bands. The PV/$\ln(O_3)$ relationship is thus used in this paper. The linear regression line with parameters β_0 and β_1 is determined by the scatterplot of SAGE II V6.1 ozone and the coincident GMAO analyzed PV. The scatterplots were made monthly on isentropic surfaces for 1999 and the relationships were derived separately for the NH and SH. The correlation coefficients between PV and $\ln(O_3)$ are provided in Table 2. It was found that the correlation between PV and ozone was low in July in the NH. This occurred because all the SAGE observations collected on these isentropic surfaces in the NH in July 1999 were located in a narrow band between 60°–70°N, where ozone had small variations and was perhaps poorly mixed. Therefore they cannot well characterize the PV and ozone relationships at midlatitudes, where the isentropic STE occurs. In practice, the PV and $\ln(O_3)$ relationships for June have been employed for July. Using these monthly PV/O_3 relationships, daily ozone distributions were derived from daily PV maps. The accuracy of the PV-mapped ozone for 1990 has been discussed by *Jing et al.* [2004] using comparisons against ozonesonde

Table 4. Estimated Annual Isentropic Ozone Fluxes in the Layer Between 330 and 370 K Across the Tropopause[a]

	NH	SH	Global
S→T	127.8 ± 36	82.4 ± 23	210.2 ± 59
T→S	58.0 ± 10	34.4 ± 6	92.4 ± 16
Net	−69.8 ± 37	−48 ± 24	−117.8 ± 61

[a]Fluxes are given in 10^9 kg yr^{-1}.

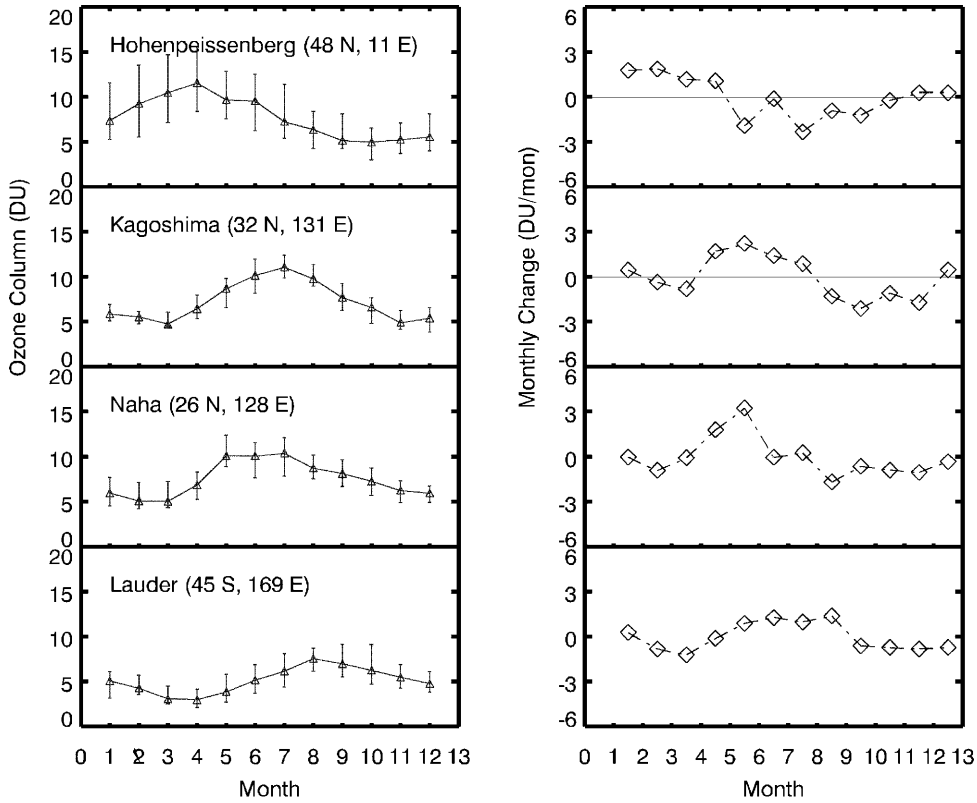

Figure 3. (left) Monthly means and (right) changes of the monthly means of the column ozone (Dobson units) in the layer between 340 and 360 K from ozonesonde observations. Error bars are percentiles.

observations. As the ozone and PV data used in this study are for a different year, similar comparisons for 1999 are shown in Table 3. It is shown that the median of the difference between the PV-mapped ozone and ozonesonde data is approximately 10%.

2.3. Calculation of Isentropic Ozone STE

[13] The calculation of isentropic ozone STE is based on contour advection. Contour advection is able to depict the continuous formation of small-scale structures in a passive tracer field following two-dimensional isentropic flows with a resolution much finer than that of the analyzed data [*Waugh and Plumb*, 1994; *Baker and Cunnold*, 2001]. Its surgery routine removes the fine-scale structures smaller than a prescribed cutoff scale δ. These cutoff small-scale structures are assumed to have been irreversibly mixed with the air in which they are now located. Contour advection with surgery has been employed to diagnose the isentropic exchange of air mass, water vapor, and ozone [*Dethof et al.*, 2000a, 2000b; *Jing et al.*, 2004] and to address the mixing during Rossby wave breaking [*Scott and Cammas*, 2002].

[14] The tropopause is defined by the PV value 3.5 PV units (PVU) (1 PVU = 10^{-6} m^2 K s^{-1} kg^{-1}) because the PV surface of 3.5 PVU best corresponds to the thermal tropopause defined by lapse rate outside the tropics [*Hoerling et al.*, 1991; *Schoeberl*, 2004]. We consider a control volume around an isentropic surface θ. The vertical boundaries of this volume are $\theta \pm 5$ K and the horizontal boundary is the tropopause. The stratosphere is located inside the volume (i.e., poleward of the tropopause) and the troposphere is outside the volume (i.e., equatorward of the tropopause). Using the quantification method based on contour advection and PV/O_3 mapping as described by *Jing et al.* [2004], daily isentropic cross-tropopause ozone fluxes both from S→T and from T→S are estimated on regular 2.5° × 2.0° (longitude by latitude) grids by calculating the ozone fluxes within the filaments formed on PV contours equatorward and poleward of the tropopause, respectively. The net ozone flux is the difference between the T→S and the S→T fluxes. For a given ozonesonde site, the daily net isentropic ozone fluxes are calculated by taking the average value of the daily net ozone fluxes on the nine horizontal grid points that are closest to that location (i.e., averaged over an area of 5° longitude by 4° latitude).

3. Estimated Isentropic Cross-Tropopause Ozone Fluxes

[15] The daily cross-tropopause ozone fluxes both from S→T and from T→S are estimated using contour advection and PV/O_3 mapping on four isentropic surfaces (i.e., 335, 345, 355, and 365 K) for 1999. The monthly average ozone fluxes and the annual ozone fluxes in both hemispheres are calculated from these daily fluxes. In this section, we study the seasonality and the interhemispheric difference of the isentropic ozone STE.

3.1. Seasonal Variations of the Isentropic Ozone STE

[16] The calculated monthly average isentropic ozone fluxes for the four isentropic surfaces between 330 and

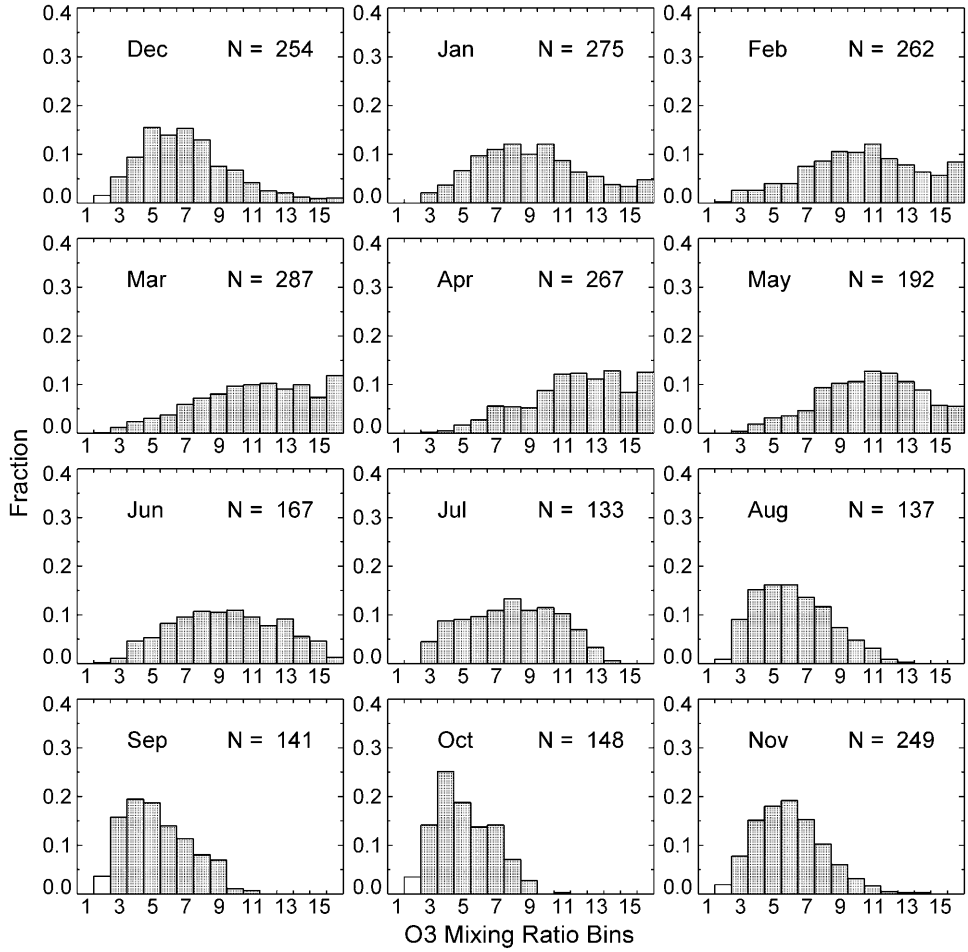

Figure 4. Distributions of ozone mixing ratio (in ppbv) within the layer between 340 and 360 K, when it is in the stratosphere, based on the observations between 1979 and 2000 over Hohenpeissenberg. N is the number of ozonesonde profiles. The sixteen ozone mixing ratio bins are 1, (0, 40]; 2, (40, 80]; 3, (80, 120]; 4, (120, 160]; 5, (160, 200]; 6, (200, 240]; 7, (240, 280]; 8, (280, 320]; 9, (320, 360]; 10, (360, 400]; 11, (400, 440]; 12, (440, 480]; 13, (480, 520]; 14, (520, 560]; 15, (560, 600]; and 16, (600, $+\infty$). Tropospheric and stratospheric ozone bins are represented by open and shaded boxes, respectively.

370 K in each hemisphere are plotted in Figure 1. Negative net isentropic fluxes indicate net S→T ozone transport and positive ones indicate net T→S ozone transport. It is shown that the S→T ozone fluxes are greater than the T→S ozone fluxes. This is not only because the isentropic flux of air mass is larger in the direction from S→T than in the direction from T→S [*Dethof et al.*, 2000a] (and confirmed in both direction and amplitude by calculations we have made for February 1990) but also because the stratospheric air has higher ozone mixing ratios than the tropospheric air [*Bethan et al.*, 1996; *P. H. Wang et al.*, 1998]. Combining those ozone fluxes on the four isentropic surfaces in Figure 1, it is shown that the estimated net ozone fluxes are directed from the extratropical LS to the subtropical UT in the layer between 330 and 370 K in every month in 1999 (Figure 2).

[17] The isentropic ozone transport displays a similar seasonality in each hemisphere. It is strongest in summer and weakest in winter (Figure 2). In the NH, both the S→T and the T→S fluxes are maximum in June/July/August (northern summer) and minimum in December/January/February (northern winter). In the SH, they are strong in January/February/March (late austral summer) and weak in June/July/August (austral winter). The seasonality of the isentropic ozone STE is opposite to that of the downward cross-tropopause diabatic ozone flux at midlatitudes, which is strongest in winter and weakest in summer [*Olsen et al.*, 2002, 2003]. This is because the two ozone STE pathways have different mixing properties. The diabatic STE is part of the Brewer-Dobson circulation, which is driven by wave-induced forces. These forces are strongest in winter, and the downward diabatic flux is therefore greatest in winter [*Holton et al.*, 1995]. On the other hand, cross-tropopause evens along isentropes are restrained in winter as indicated by the large PV gradients in the vicinity of the jet stream. In summer, however, the cross-tropopause activity along isentropes increases because the jet stream is weaker [*Holton*, 1992; *Chen*, 1995; *Haynes and Shuckburgh*, 2000]. The ozone-rich air, which has been dumped into the extratropical LS from higher altitudes in winter, will spread quasi-

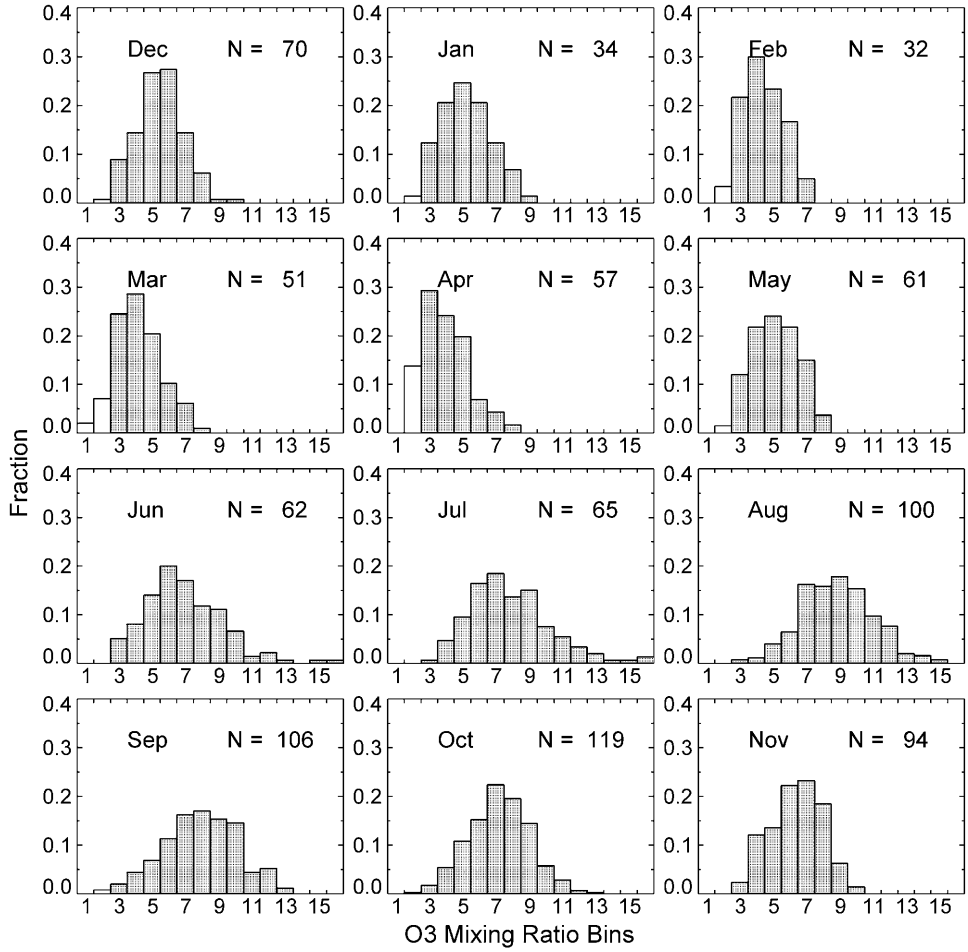

Figure 5. Similar to Figure 4 but for the observations between 1986 and 2000 over Lauder.

horizontally into the subtropical UT via isentropic transport in summer.

3.2. Interhemispheric Difference in the Estimated Annual Isentropic Ozone Fluxes

[18] Although the seasonal phase of the isentropic ozone STE is similar in both hemispheres, it is noted that the estimated annual ozone fluxes (both from S→T and from T→S) are more than 50% greater in the NH than in the SH (Table 4). For the S→T flux, this is mainly because the ozone mixing ratios in the LS in the NH are greater than in the SH [*P. H. Wang et al.*, 1998], and the transport of reduced springtime ozone air from high latitudes in the SH is likely to be one of the reasons that ozone mixing ratios in the SH lower stratosphere are lower than those in the NH. There may also be a contribution from a greater number of Rossby wave breaking events in the NH than in the SH [*Postel and Hitchman*, 1999] and the subtropical UT and extratropical LS are therefore better mixed in the NH. Globally, the annual T→S ozone flux is estimated to be 92 ± 16 Tg yr^{-1} and the annual S→T flux is 210 ± 59 Tg yr^{-1}. The net amount of ozone that is transported globally into the subtropical UT is 118 ± 61 Tg yr^{-1}. The error bars reflect the major uncertainties in the estimates [see *Jing et al.*, 2004]: a possible bias (±10%) of the PV-mapped ozone, an uncertainty (±5%) induced by a change of ±60 km in the cutoff scale used in the surgery routine of contour advection, and an uncertainty (±26% in S→T; ±13% in T→S) resulting from ±1 PVU in the tropopause definition.

[19] It is noted that the estimated net annual S→T ozone flux in the NH in this paper (Table 4) is approximately 40% higher than the value (∼50 Tg yr^{-1}) given by *Jing et al.* [2004]. There are two main reasons for the difference. One is that we have used different assimilation data set in this paper (GEOS-3 for the year 1999) whereas *Jing et al.* [2004] used GEOS-1 for the year 1990. Another important reason is that observed ozone mixing ratios (both from SAGE II and from ozonesondes at Hohenpeissenberg) at midlatitudes in the northern LS are ∼20% higher in 1999 than in 1990 (not shown in this paper). *Hood et al.* [1997] showed that the negative total column ozone anomalies at 45°N in 1990 could have been due to horizontal advective transport from the subtropics.

4. Seasonal Variations of Ozone From Ozonesonde Observations

[20] The seasonality of isentropic ozone STE would tend to increase ozone levels in the subtropical UT in spring and summer, particularly in the NH (Figure 2). Monthly ozone columns in the layer between 340 and 360 K have therefore been calculated using ozonesonde observations over Hohen-

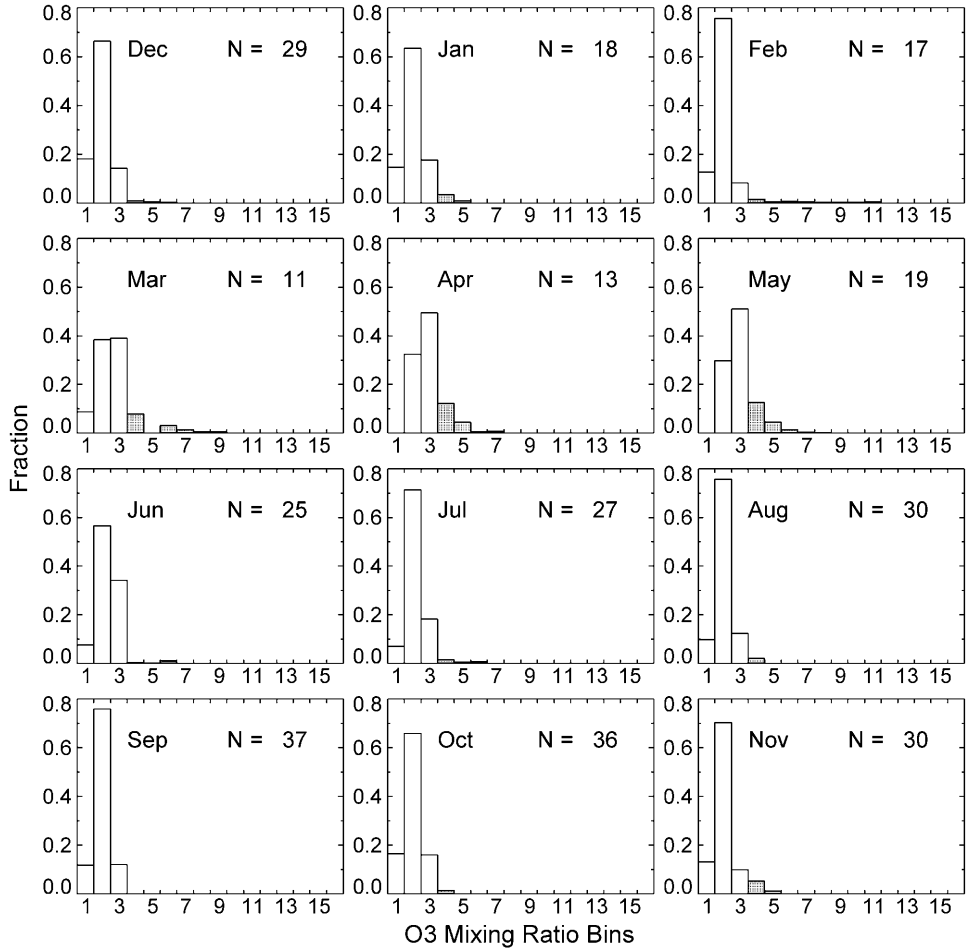

Figure 6. Similar to Figure 4 but for the observations between 1991 and 2001 over Kagoshima when the 340–360 K layer is in the troposphere. Note that the scale of the *y* axis is different from those in Figures 4 and 5.

peissenberg (1979–2001), Lauder (1986–2000), Kagoshima (1991–2000), and Naha (1991–2000). Their seasonal variations are shown in Figure 3. The layer between 340 and 360 K is chosen rather than 330 and 370 K because the 340–360 K layer is usually located in the extratropical LS over Hohenpeissenberg and Lauder and in the subtropical UT over Kagoshima and Naha. For the calculations in Figures 3–7, we excluded cases in which the thermal tropopause was above 340 K over the first two ozonesonde stations or when the thermal tropopause was below 360 K over the latter two. The calculations and presented values therefore are not influenced by the effects of the seasonal cycle in the height of the tropopause. Overall, approximately 10% of the total profiles were excluded for each station, and ~30% of the summer profiles were excluded over Hohenpeissenberg and Lauder. The layer ozone between 340 and 360 K in the extratropical LS (i.e., over Hohenpeissenberg and Lauder) is largest in spring and smallest in fall, while the layer ozone in the subtropical UT (i.e., over Kagoshima and Naha) is largest in summer and smallest in winter. The seasonal trends of the layer ozone over Kagoshima and Naha are of about the same magnitude but of opposite sign to those over the LS stations. The seasonality is consistent with the concept that ozone first increases in the extratropical LS in winter because of the strong diabatic downward flux and it then spreads into the subtropical UT via isentropic transport in summer. The increase of ozone levels in the UT starts almost immediately after the PV gradient around the tropopause weakens, probably because isentropic STE occurs relatively rapidly, on a timescale of days to weeks [*Chen*, 1995].

[21] *P. H. Wang et al.* [1998], using SAGE II measurements, showed spring to summer ozone decreases in the LS extratropics and ozone increases in the subtropics in the NH, of similar magnitude to those in Figure 3, without the restriction that the 340–360 K was in the LS for the extratropics or in the UT for the subtropics. They also discussed these changes in terms of isentropic ozone STE but without quantitative estimates of the effect. They showed that the monthly mean height of the 340–360 K layer above the tropopause possessed a relatively insignificant seasonal variation, less than approximately 1 km. Therefore there is little impact on the 340–360 K layer from the vertical movement of the layer relative to the tropopause. Furthermore, they demonstrated that seasonal changes in layer thickness (in their case, for the 330–380 K layer) made only a small contribution to the ozone changes. Both *P. H. Wang et al.* [1998] and the Lauder ozonesonde data indicate smaller ozone changes in the southern LS than in the northern LS in late spring/early

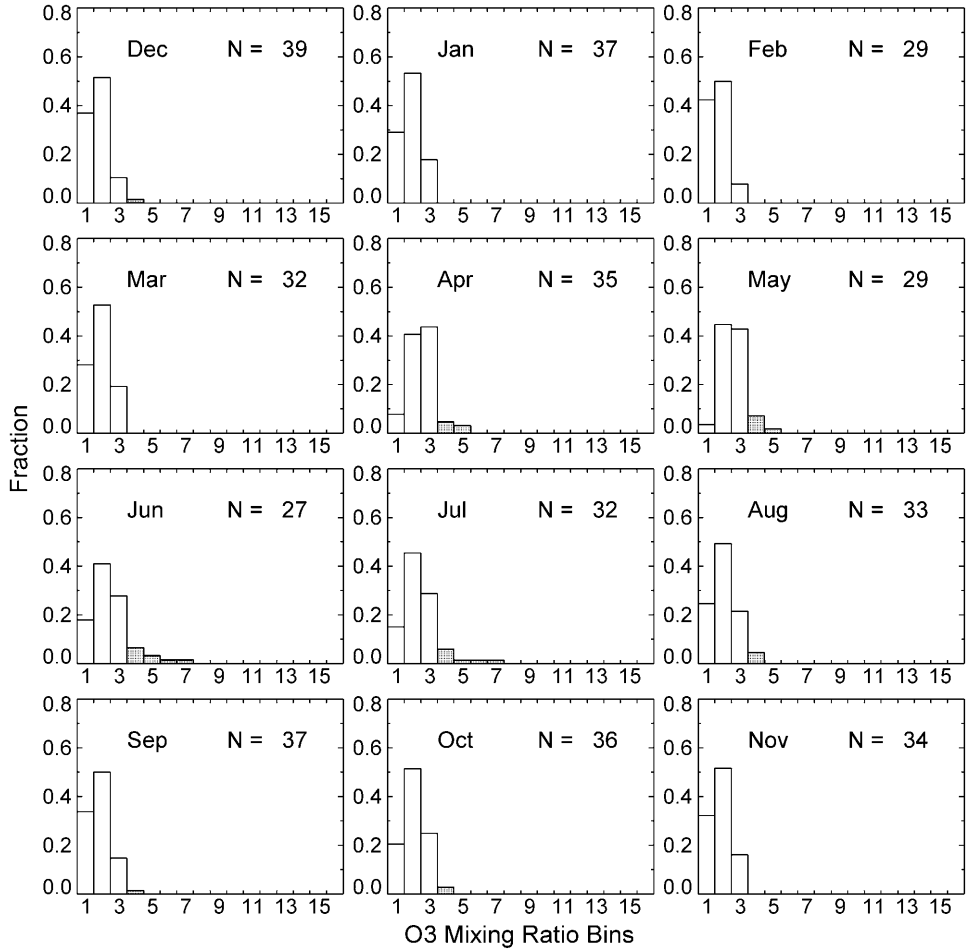

Figure 7. Similar to Figure 6 but for the observations between 1991 and 2000 over Naha.

summer (i.e., November/December/January in the SH and May/June/July in the NH). This may be, at least in part, the result of dilution of LS ozone at SH midlatitudes produced by the spreading of reduced ozone following the break up of the Antarctica vortex.

[22] The monthly distributions of the observed ozone mixing ratios within the 340–360 K layer for Hohenpeissenberg, Lauder, Kagoshima, and Naha are shown in Figures 4–7. Ozone mixing ratios greater than 110 ppbv are considered to have stratospheric origin for the subtropical UT locations, and ozone mixing ratios less than 80 ppbv are of tropospheric origin for the extratropical LS locations, based on the definition of the ozone tropopause given by *Bethan et al.* [1996]. Figures 4–7 then confirm that, for the profiles studied, the 340–360 K layer ozone is mostly of stratospheric origin over Hohenpeissenberg and Lauder (Figures 4 and 5) and of tropospheric origin over Kagoshima and Naha (Figures 6 and 7). During summer, there are increasing cases of ozone mixing ratio <80 ppbv over Lauder (Figure 5), indicating the influence of some T→S transport from the UT. These T→S transport cases could have been associated with isentropic transport because the diabatic upward T→S transport occurs mainly in the subtropics/tropics [*Holton et al.*, 1995; *Schoeberl*, 2004].

[23] In comparison, there are more ozone mixing ratios >110 ppbv observed during late spring and early summer over Kagoshima and Naha (Figures 6 and 7), suggesting the influence of S→T transport from the LS. Because the downward diabatic ozone flux between 30° and 60° latitude decreases rapidly during this time of the year [*Olsen et al.*, 2002, 2003], these S→T transport cases are probably isentropic. For example, on 16 June 1999 the observed ozone profile at Naha shows an ozone peak (>110 ppbv and thus considered to be stratospheric) around 360 K and this ozone peak is located in the troposphere according to the temperature profile (Figure 8). At the same time, the PV field at 360 K from contour advection calculations demonstrates that there is a stream of stratospheric air with PV > 3.5 PVU over Naha (Figure 9), indicating the influence of isentropic S→T transport. It should be noted that the histograms over Kagoshima show a tail of stratospheric ozone bins in spring. This may be because the 340–360 K layer over Kagoshima is 6° of latitude farther north than Naha and it is in the vicinity of the subtropical jet stream in spring. Stratospheric air could be transported into the subtropical UT quasi-horizontally in the vicinity of the jet stream [*Tuck et al.*, 2003].

[24] For 1999, we have calculated the isentropic cross-tropopause ozone fluxes over Kagoshima and Naha using the contour advection procedure. They are found to be 0.5 ∼ 1.5 DU month^{-1} over Naha and 2 ∼ 3 DU month^{-1} over Kagoshima in May and June 1999 (Figure 10). Maximum downward diabatic fluxes occur in winter [*Olsen et al.*, 2002,

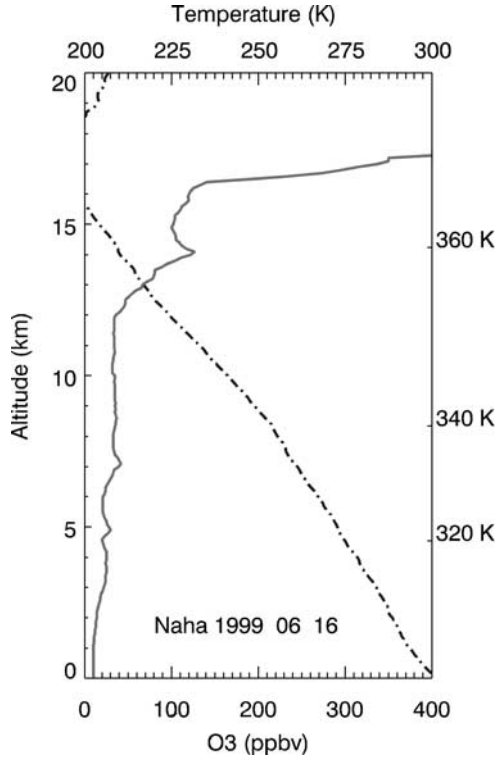

Figure 8. Ozone (shaded) and temperature (dash-dotted) profiles over Naha on 16 June 1999.

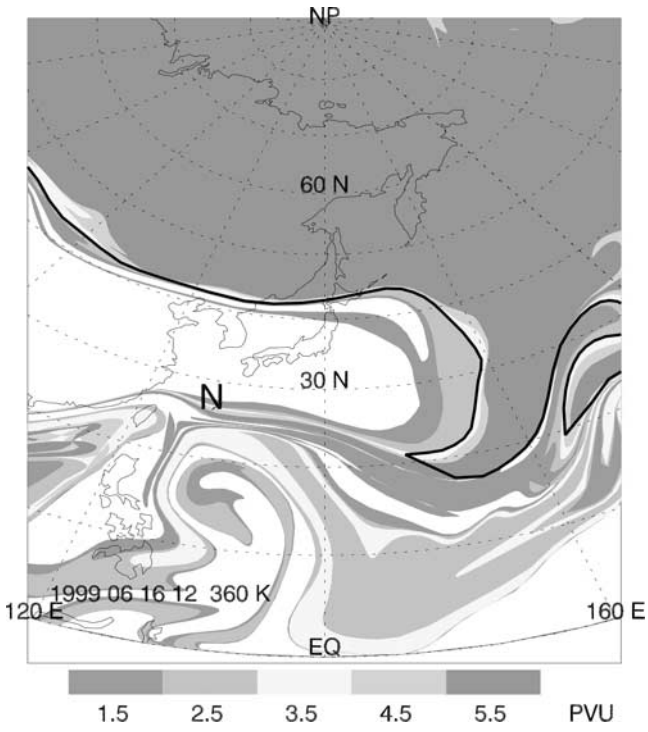

Figure 9. Potential vorticity field at 360 K on 16 June 1999 at 1200 UTC after 5 day contour advection calculations. The bold black line represents the 3.5 PV units tropopause determined by the surgery routine of contour advection. "N" represents the location of Naha. See color version of this figure at back of this issue.

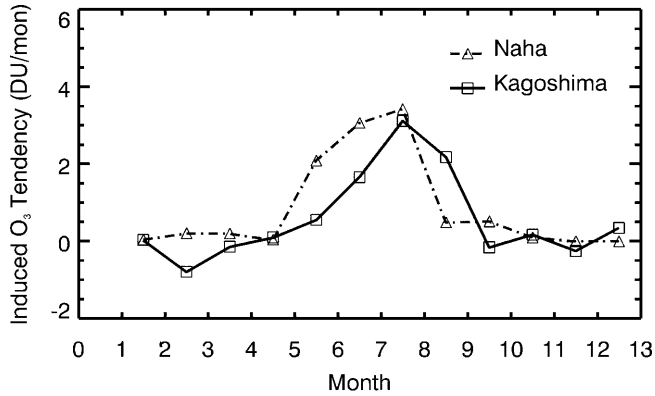

Figure 10. Estimated monthly ozone tendencies between 340 and 360 K over Kagoshima and Naha in 1999 due to the net isentropic S→T transport.

2003] and therefore the observed maximum ozone increase in the subtropical UT in late spring may be caused by isentropic motions which maximize at that time of year. In contrast, *Y. Wang et al.* [1998] have calculated the zonally averaged rate for net photochemical ozone production in July around 30° N above 200 hPa to be ~0.5 ppbv d^{-1} (~0.3 DU km^{-1} $month^{-1}$). In the 340–360 K layer, which is 2 ~ 4 km thick, photochemistry would thus provide a column ozone source of 0.6 ~ 1.2 DU $month^{-1}$ at the latitudes of Kagoshima and Naha. On the basis of our calculations, this suggests that isentropic ozone transport makes a significant contribution to UT ozone changes in the subtropics in summer.

5. Discussion and Conclusion

[25] Isentropic cross-tropopause ozone fluxes between 330 and 370 K have been estimated using contour advection and SAGE ozone measurements. The estimated ozone fluxes both from the stratosphere-to-troposphere (S→T) and from the troposphere-to-stratosphere (T→S) are strongest in summer and weakest in winter. The net isentropic ozone flux is directed from S→T and it is also the greatest in summer. Although both hemispheres display similar seasonality of the isentropic ozone transport, the ozone fluxes in the Northern Hemisphere (NH) are approximately 50% greater than those in the Southern Hemisphere (SH). This is mainly because the lower stratosphere in the NH has higher ozone mixing ratios than in the SH [*P. H. Wang et al.*, 1998]. It may also be because there are more Rossby wave breaking events in the NH than in the SH [*Postel and Hitchman*, 1999]. The potential effect of the isentropic mixing around the tropopause is to increase ozone concentrations in the subtropical/tropical upper troposphere (UT) and decrease them in the extratropical lower stratosphere (LS) and this effect should be more pronounced in summer than in winter.

[26] The tropopause crosses the isentropic surfaces between 330 and 370 K in the subtropics. The results in this paper thus reflect the isentropic cross-tropopause transport of ozone between the LS and subtropical/tropical UT. We have not considered the isentropic surfaces lower than 330 K, which would intersect with the tropopause at higher latitudes. The direction and magnitude of the isentropic ozone flux

below 330 K is not clear. It has been indicated that air could be transported from the UT to the LS isentropically in subpolar regions [*Hoerling et al.*, 1993]. However, the net isentropic ozone flux might still be from S→T, because of the large ozone mixing ratio gradient between the LS and UT.

[27] The net amount of ozone transported across the tropopause into the subtropical/tropical UT is estimated to be 118 ± 61 Tg yr^{-1} in this study. It should be noted, however, that this uncertainty range might be underestimated. The contour advection technique has limited ability to capture all the small-scale structures that evolve near the tropopause in the UT. Local dynamical processes might not be well depicted by contour advection using coarse-resolution wind fields, and PV contours might be eroded by sporadically strong diabatic heating in the UT [*Bithell et al.*, 1999; *Shepherd et al.*, 2000].

[28] According to *Houghton et al.* [2001], present model estimates of the total stratospheric source of the tropospheric ozone are 400 ∼ 1000 Tg yr^{-1}. From a global and annual viewpoint, diabatic processes seem to dominate the exchange of ozone. However, for the regions where the isentropic ozone STE mostly occurs (i.e., over the northern Pacific and Atlantic Oceans and northwest Africa), the isentropic transport of ozone may be larger than the diabatic ozone transport and be regionally important.

[29] The observed seasonal variations of ozone within the isentropic layer between 340 and 360 K have been analyzed using ozonesonde data. Over those extratropical stations such as Hohenpeissenberg in Germany and Lauder in New Zealand, ozone within the 340–360 K layer is mostly stratospheric. Ignoring those days when this layer is not completely in the stratosphere, maximum ozone in this layer is found in spring and the minimum is in the fall, and most cases of ozone of tropospheric origin (<80 ppbv) are observed in late summer. This may suggest the influence of isentropic T→S flow from the subtropics. Over the subtropical stations such as Kagoshima and Naha in Japan, ozone within the 340–360 K layer is mostly tropospheric; ozone in this layer is highest in summer and lowest in winter; and increasing cases of stratospheric ozone (>110 ppbv) are observed in early summer. On the basis of our calculated isentropic ozone STE fluxes in the layer above these two sites, and the reported magnitude of the photochemical source, it is unlikely that photochemistry alone can explain the seasonality and variability in ozone. We conclude that the isentropic ozone exchange across the tropopause is an important source for ozone in the subtropical/tropical upper troposphere during summertime.

[30] **Acknowledgments.** The authors would like to thank Darryn Waugh for providing the contour advection code and Mark Olsen for his helpful discussions. Thanks to Gi-Kong Kim and the NASA Global Model and Assimilation Office for supplying the GEOS-3 assimilated meteorological data for 1999 as a limited release. This work has been supported by NASA contracts NAG1-2202, NAS5-00171, NAS1-96016, and NNG-04GC87G.

References

Appenzeller, C., H. C. Davies, and W. A. Norton (1996), Fragmentation of stratospheric intrusions, *J. Geophys. Res.*, *101*, 1435–1456.

Baker, M. N., and D. M. Cunnold (2001), On the uses and limitations of contour advection as a technique for understanding vortex dynamics, *J. Atmos. Sci.*, *58*, 2210–2221.

Bethan, S., G. Vaughan, and S. J. Reid (1996), A comparison of ozone and thermal tropopause heights and the impact of tropopause definition on quantifying the ozone content of the troposphere, *Q. J. R. Meteorol. Soc.*, *122*, 929–944.

Bithell, M., L. J. Gray, and B. D. Cox (1999), Three-dimensional view of the evolution of midlatitude stratospheric intrusions, *J. Atmos. Sci.*, *56*, 673–688.

Chen, P. (1995), Isentropic cross-tropopause mass exchange in the extratropics, *J. Geophys. Res.*, *100*, 16,661–16,673.

Danielson, E. F. (1968), Stratospheric-tropospheric exchange based on radioactivity, ozone and potential vorticity, *J. Atmos. Sci.*, *25*, 502–518.

Danielson, E. F., R. S. Hipskind, S. E. Gaines, G. W. Sachse, G. L. Gregory, and G. F. Hill (1987), Three-dimensional analysis of potential vorticity associated with tropopause folds and observed variations of ozone and carbon monoxide, *J. Geophys. Res.*, *92*, 2103–2111.

Data Assimilation Office (1997), GEOS-3 data assimilation system architectural design, *DAO Off. Notes 97–06*, NASA Goddard Space Flight Cent., Greenbelt, Md.

Davis, D. D., et al. (2003), An assessment of western North Pacific ozone photochemistry based on springtime observations from NASA's PEM-West B (1994) and TRACE-P (2001) field studies, *J. Geophys. Res.*, *108*(D21), 8829, doi:10.1029/2002JD003232.

Dessler, A. E., E. J. Hintsa, G. M. Weinstock, J. G. Anderson, and K. R. Chan (1995), Mechanisms controlling water vapor in the lower stratospheres: "A tale of two stratospheres", *J. Geophys. Res.*, *100*, 23,167–23,172.

Dethof, A., A. O'Neill, and J. Slingo (2000a), Quantification of the isentropic mass transport across the dynamical tropopause, *J. Geophys. Res.*, *105*, 12,279–12,293.

Dethof, A., A. O'Neill, J. Slingo, and P. Berrisford (2000b), Quantification of isentropic water vapor transport into the lower stratosphere, *Q. J. R. Meteorol. Soc.*, *126*, 1771–1788.

Edouard, S., R. Vautard, and G. Brunet (1997), On the maintenance of potential vorticity in isentropic coordinates, *Q. J. R. Meteorol. Soc.*, *123*, 2069–2094.

Gettelman, A., J. R. Holton, and K. H. Rosenlof (1997), Mass fluxes of O_3, CH_4, N_2O and CF_2Cl_2 in the lower stratosphere calculated from observational data, *J. Geophys. Res.*, *102*, 19,149–19,159.

Gidel, L. T., and M. A. Shapiro (1980), General circulation model estimates of the net vertical flux of ozone in the lower stratosphere and the implications for the tropospheric ozone budget, *J. Geophys. Res.*, *85*, 4049–4058.

Haynes, P., and E. Shuckburgh (2000), Effective diffusivity as a diagnostic of atmospheric transport. Part II: Troposphere and lower stratosphere, *J. Geophys. Res.*, *105*, 22,795–22,810.

Hoerling, M. P., T. K. Schaack, and A. J. Lenzen (1991), Global objective tropopause analysis, *Mon. Weather Rev.*, *119*, 1816–1831.

Hoerling, M. P., T. K. Schaack, and A. J. Lenzen (1993), A global analysis of stratosphere-troposphere exchange during northern winter, *Mon. Weather Rev.*, *121*, 162–172.

Holton, J. R. (1992), *An Introduction to Dynamic Meteorology*, 511 pp., Elsevier, New York.

Holton, J. R., P. H. Hayns, M. E. McIntyre, A. R. Douglass, R. B. Rood, and L. Pfister (1995), Stratosphere-troposphere exchange, *Rev. of Geophys*, *33*, 403–439.

Hood, L. L., J. P. McCormack, and K. Labitzke (1997), An investigation of dynamical contributions to midlatitude ozone trend in winter, *J. Geophys. Res.*, *102*, 13,079–13,093.

Hoskins, B. J. (1991), Towards a PV–θ view of the general circulation, *Tellus, Ser. A*, *43AB*, 27–35.

Intergovernmental Panel on Climate Change (2001), *Climate Change 2001: The Scientific Basis—Contribution of Working Group I to the Third Assessment Report of IPCC*, edited by J. T. Houghton et al., 944 pp., Cambridge Univ. Press, New York.

Jing, P., D. M. Cunnold, H.-J. Wang, and E.-S. Yang (2004), Isentropic cross-tropopause ozone transport in the Northern Hemisphere, *J. Atmos. Sci.*, *61*, 1068–1078.

Junge, C. E. (1962), Global ozone budget and exchange between stratosphere and troposphere, *Tellus*, *14*, 363–377.

Morgenstern, O., and G. D. Carver (2001), Comparison of cross-tropopause transport and ozone in the upper troposphere and lower stratosphere region, *J. Geophys. Res.*, *106*, 10,205–10,221.

Morgenstern, O., and A. Marenco (2000), Wintertime climatology of MOZAIC ozone based on the potential vorticity and ozone analogy, *J. Geophys. Res.*, *105*, 15,481–15,493.

Müller, J. F., and G. P. Brasseur (1995), IMAGES: A three–dimensional chemical-transport model of the global troposphere, *J. Geophys. Res.*, *100*, 16,445–16,490.

Murphy, D. M., and D. W. Fahey (1994), An estimate of the flux of stratospheric reactive nitrogen and ozone in the troposphere, *J. Geophys. Res.*, *99*, 5325–5332.

Olsen, M. A., A. R. Douglass, and M. R. Schoeberl (2002), Estimating downward cross-tropopause ozone flux using column ozone and potential vorticity, *J. Geophys. Res.*, *107*(D22), 4636, doi:10.1029/2001JD002041.

Olsen, M. A., A. R. Douglass, and M. R. Schoeberl (2003), A comparison of Northern Hemisphere and Southern Hemisphere cross-tropopause ozone flux, *Geophys. Res. Lett.*, *30*(7), 1412, doi:10.1029/2002GL016538.

Postel, A. P., and M. H. Hitchman (1999), A climatology of Rossby wave breaking along the subtropical tropopause, *J. Atmos. Sci.*, *56*, 359–373.

Price, J. D., and G. Vaughan (1993), On the potential for stratosphere-troposphere exchange in cut-off low systems, *Q. J. R. Meteorol. Soc.*, *119*, 343–365.

Schoeberl, M. R. (2004), Extratropical stratosphere-troposphere mass exchange, *J. Geophys. Res.*, *109*, D13303, doi:10.1029/2004JD004525.

Scott, R. K., and J.-P. Cammas (2002), Wave breaking and mixing at the subtropical tropopause, *J. Atmos. Sci.*, *59*, 2347–2361.

Seo, K. H., and K. P. Bowman (2001), A climatology of isentropic cross-tropopause exchange, *J. Geophys. Res.*, *106*, 28,159–28,172.

Shepherd, T. G., J. N. Koshyk, and N. Ngan (2000), On the nature of large-scale mixing in the stratosphere and mesosphere, *J. Geophys. Res.*, *105*, 12,433–12,446.

Tuck, A. F., et al. (1997), The Brewer-Dobson circulation in the light of high altitude in situ aircraft observations, *Q. J. R. Meteorol. Soc.*, *123*, 1–69.

Tuck, A. F., S. J. Hovde, K. K. Kelly, M. J. Mahoney, M. H. Proffitt, E. C. Richard, and T. L. Thompson (2003), Exchange between the upper tropical troposphere and the lower stratosphere studied with aircraft observations, *J. Geophys. Res.*, *108*(D23), 4734, doi:10.1029/2003JD003399.

Wang, H.-J., D. M. Cunnold, L. M. Thomason, J. M. Zawodny, and G. E. Bodeker (2002), Assessment of SAGE version 6.1 ozone data quality, *J. Geophys. Res.*, *107*(D23), 4691, doi:10.1029/2002JD002418.

Wang, P. H., J. M. Zawodny, R. B. Pierce, J. R. Olson, G. S. Kent, and K. M. Skeens (1998), Seasonal ozone variations in the isentropic layer between 330 and 380K as observed by SAGE II: Implications of extratropical cross-tropopause transport, *J. Geophys. Res.*, *103*, 28,647–28,659.

Wang, Y., D. J. Jacob, and J. A. Logan (1998), Global simulation of tropospheric O_3-NO_x-hydrocarbon chemistry: 3. Origin of tropospheric ozone and effects of nonmethane hydrocarbons, *J. Geophys. Res.*, *103*, 10,757–10,767.

Waugh, D. W., and R. A. Plumb (1994), Contour advection with surgery: A technique for investigating fine scale structure in tracer transport, *J. Atmos. Sci.*, *51*, 530–540.

Waugh, D. W., et al. (1997), Mixing of polar vortex air into middle latitudes as revealed by tracer-tracer scatterplots, *J. Geophys. Res.*, *102*, 13,119–13,134.

Zachariasse, M., P. F. J. van Velthoven, H. G. J. Smit, J. Lelieveld, T. K. Mandal, and H. Kelder (2000), Influence of stratosphere-troposphere exchange on tropospheric ozone over the tropical Indian Ocean during the winter monsoon, *J. Geophys. Res.*, *105*, 15,403–15,416.

D. M. Cunnold, P. Jing, H.-J. Wang, and E.-S. Yang, School of Earth and Atmosphere Sciences, Georgia Institute of Technology, 311 Ferst Drive, Atlanta, GA 30332-0340, USA. (pjing@eas.gatech.edu)

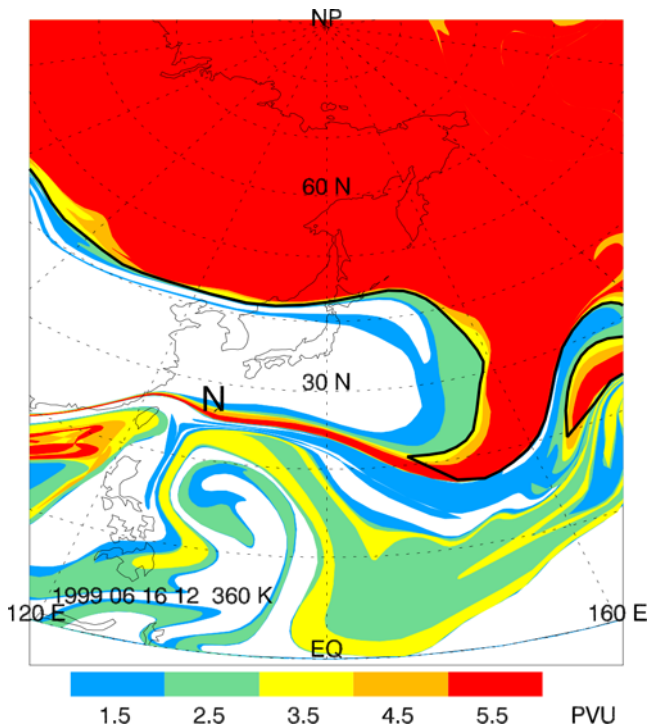

Figure 9. Potential vorticity field at 360 K on 16 June 1999 at 1200 UTC after 5 day contour advection calculations. The bold black line represents the 3.5 PV units tropopause determined by the surgery routine of contour advection. "N" represents the location of Naha.